

# Strength and deformability of wide flange beams connected to RHS-column

Autor(en): **Inoue, Kazuo / Wakiyama, Koza / Tateyama, Eiji**

Objektyp: **Article**

Zeitschrift: **IABSE congress report = Rapport du congrès AIPC = IVBH  
Kongressbericht**

Band (Jahr): **13 (1988)**

PDF erstellt am: **27.07.2024**

Persistenter Link: <https://doi.org/10.5169/seals-13068>

## **Nutzungsbedingungen**

Die ETH-Bibliothek ist Anbieterin der digitalisierten Zeitschriften. Sie besitzt keine Urheberrechte an den Inhalten der Zeitschriften. Die Rechte liegen in der Regel bei den Herausgebern.

Die auf der Plattform e-periodica veröffentlichten Dokumente stehen für nicht-kommerzielle Zwecke in Lehre und Forschung sowie für die private Nutzung frei zur Verfügung. Einzelne Dateien oder Ausdrucke aus diesem Angebot können zusammen mit diesen Nutzungsbedingungen und den korrekten Herkunftsbezeichnungen weitergegeben werden.

Das Veröffentlichen von Bildern in Print- und Online-Publikationen ist nur mit vorheriger Genehmigung der Rechteinhaber erlaubt. Die systematische Speicherung von Teilen des elektronischen Angebots auf anderen Servern bedarf ebenfalls des schriftlichen Einverständnisses der Rechteinhaber.

## **Haftungsausschluss**

Alle Angaben erfolgen ohne Gewähr für Vollständigkeit oder Richtigkeit. Es wird keine Haftung übernommen für Schäden durch die Verwendung von Informationen aus diesem Online-Angebot oder durch das Fehlen von Informationen. Dies gilt auch für Inhalte Dritter, die über dieses Angebot zugänglich sind.

## Strength and Deformability of Wide Flange Beams Connected to RHS Column

Résistance et déformation de poutres à larges ailes fixées à des colonnes RHS

Festigkeit und Verformbarkeit von Breitflanschträgern verbunden mit RHS-Stützen

### **Kazuo INOUE**

Assistant  
Osaka Univ.  
Osaka, Japan

### **Kozo WAKIYAMA**

Assoc, Prof.  
Osaka Univ.  
Osaka, Japan

### **Eiji TATEYAMA**

Lecturer  
Kinki Univ.  
Osaka, Japan

### **Hiromichi MATSUMURA**

Maneger  
NKK Building Techn. Lab.  
Kawasaki, Japan

### **SUMMARY**

This paper deals with the flexural strength and deformability of beams at the rigid frame connection with diaphragms. An improved detail of the connection is proposed without scallops (rat holes) which are conventionally provided at the beam end. From test and analytical results, it has been confirmed that the non-scallop type of connection has advantages over the scallop type with regard to strength, deformability and fabrication costs.

### **RÉSUMÉ**

Ce rapport traite de résistance à la flexion et des déformations de poutres en acier à larges ailes, fixées rigidement à une colonne RHS. La technique de raccordement décrite dans ce rapport, dans laquelle on ne fait pas appel à des pièces de recouvrement, permet d'accroître la résistance à la flexion et de diminuer la déformation tout en réduisant les coûts de fabrication.

### **ZUSAMMENFASSUNG**

Dieser Beitrag berichtet über die Ergebnisse, die bei Experimenten und Analysen an mit RHS-Stützen fest verbundenen Breitflanschträgern hinsichtlich der Biegefestigkeit und der Verformbarkeit an den Verbindungsstellen gewonnen wurden. In dieser Schrift wird der vollflächige Anschluss empfohlen, bei dem im Gegensatz zu konventionellen Verfahren mit Ausklinkungen im Steg an den Trägerenden die Biegefestigkeit und die Verformbarkeit der Träger nicht abnimmt und Konstruktionskosten eingespart werden können.



## 1. INTRODUCTION

In Japan, the rigid frame connections consisting of RHS columns and wide flange beams are generally constructed as shown in Fig.1. For this type of connection, it is technically difficult to construct the web continuation within the RHS column. Therefore, the beam web is practically semi-rigidly connected. Thus the bending strength transferred by the web is smaller than the full plastic moment of web section due to the external deformation of the column tube wall.

For the connections shown in Fig.1, the scallops (rat holes) are usually cut at the end of the beam web to avoid weld lines from intersection and to install the backing strip. The most effective part of the beam web which carries both moment and shear is lost by these scallops. Besides, the strain of the tensile flange concentrates on the scalloped part; the beam fails to tear the tensile flange [1,2]. This type of fracture has also been seen in the present research.

To improve the weak points of the conventional scalloped connection mentioned above, a nonscallop detail is designed. The flexural strength and deformability of beams connected without scallops examined through two types of specimens: one is a simple beam type, and the other is a cruciform subassemblage. Test results are compared with those of the tests on the scalloped specimens. The results of calculation on the flexural strength of beams based on the yield line theory of limit analysis is also presented.

## 2. TEST SPECIMENS AND DETAIL OF BEAM-TO-COLUMN CONNECTION

### 2.1 Test Specimens

Two types of specimens are shown in Fig.2 and Fig.3, respectively. Loading conditions are also shown in Figs.2 and 3. The cruciform subassemblages are subjected to repeated load which corresponds to the earthquake type of loading. During the loading, the joint and the application points of forces on both beam ends are so controlled as to stay in one straight line as shown in Fig.4.

Each specimen is summarized in Table 1. The nine specimens from No.1 through No.9 are the simple beam type and the specimens No.10 and No.11 are the cruciform subassemblage. The specimens of each kind include both scallop and

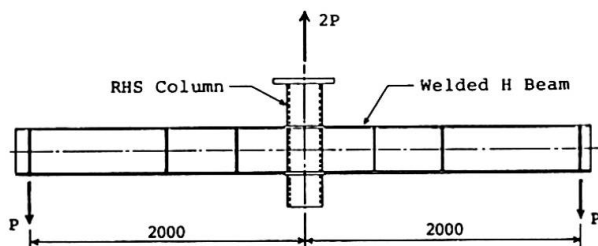


Fig.2 Simple beam specimen

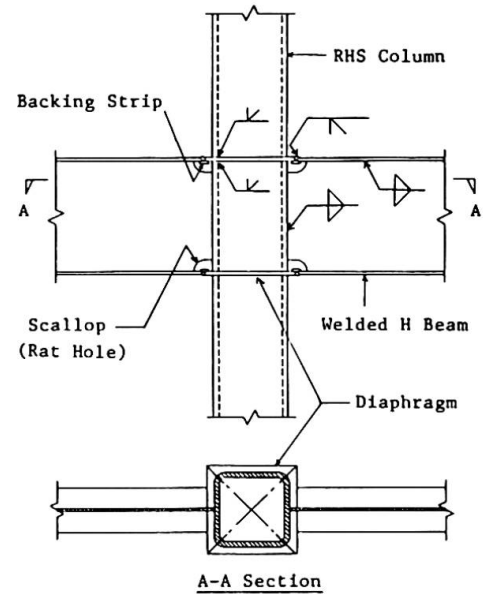


Fig.1 Wide flange beam-to-RHS column connection

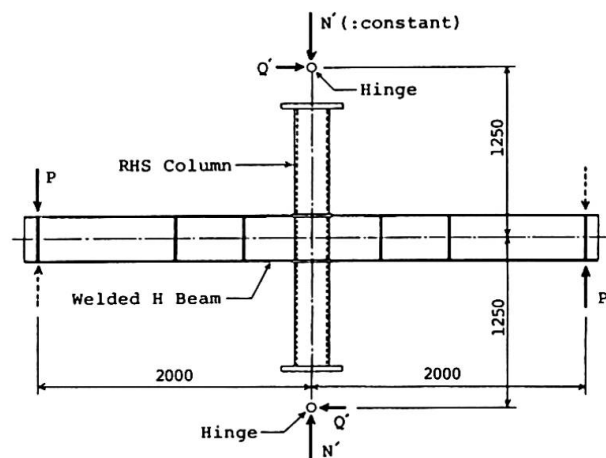


Fig.3 Cruciform subassemblage

No.	Designation	Beam	Column	Note
1	SB6-S-2A	Welded H section with two axes of symmetry	□-250 <sup>2</sup> x6	with scallop
2	SB9-S-2A		□-250 <sup>2</sup> x9	
3	SB12-S-2A		□-250 <sup>2</sup> x12	
4	SB6-N-2A	with a single axis of symmetry	□-250 <sup>2</sup> x6	non-scallop
5	SB9-N-2A		□-250 <sup>2</sup> x9	
6	SB12-N-2A		□-250 <sup>2</sup> x12	
7	SB6-S-1A	with two axes of symmetry	□-250 <sup>2</sup> x6	with scallop
8	SB6-N-1A		□-250 <sup>2</sup> x6	
9	SB12-N-1A		□-250 <sup>2</sup> x12	
10	CS12-S-2A	with two axes of symmetry	□-250 <sup>2</sup> x12	with scallop
11	CS12-N-2A		□-250 <sup>2</sup> x12	

Table 1 Summary of test specimens

nonscallop type of connections. All columns are cold-formed RHS tubes. Beams are welded wide flange steel beams; some having the section with two axes of symmetry and the others having the section with a single axis of symmetry as shown in Fig.5 (a) and (b). In the case of the composite beam subjected to positive bending, the plastic neutral axis lies inside or outside but near the upper flange of steel beam. The specimens No.7 through No.9 with a single axis of symmetry are prepared for examining the flexural strength and deformability of steel beam in the composite beam. Both of the two cruciform specimens are composed of beams with two axes of symmetry shown in Fig.5 (a). Specimen No.10 has scallops and Specimen No.11 is of the nonscallop type.

## 2.2 Detail of Nonscallop Connection

The detail of the scalloped connection is shown in Fig.6. The welding process of the nonscalloped connection is shown in Fig.7(a)-(c). This process is applicable only to the welded wide flange beams and is summarized as follows:

- (1) The fillet welding of the flange and the web into a wide flange beam is suspended at point A as shown by Fig.7 (a) to install the backing strips. Next, the end corner of beam web is cut in such a shape as to fit the reinforcement of the butt joint of the diaphragm and the RHS column.
- (2) Two backing strips are installed, on both side of the web as shown in Fig.7 (b) and (c). They are fillet welded to the diaphragm and to the beam flange. Next, the diaphragm and beam flange are butt welded.
- (3) As shown in Fig.7 (b), the fillet welding is started from Point A to connect the beam web and the RHS column.

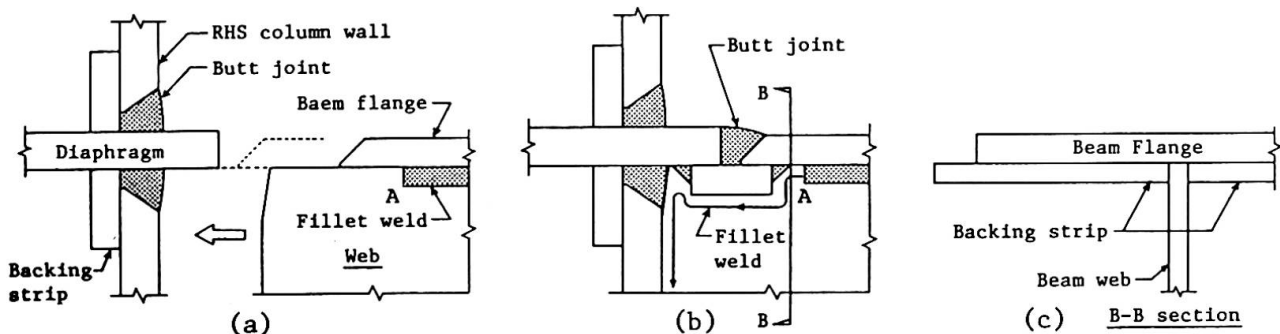


Fig.7 Welding process of nonscalloped connection

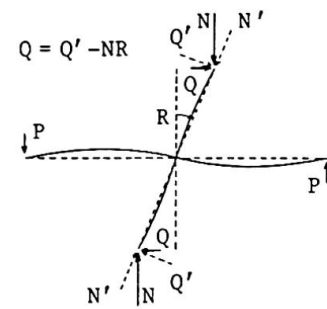


Fig.4

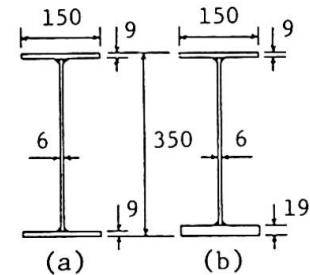


Fig.5 Beam section

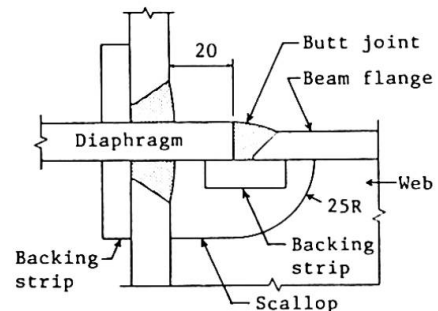


Fig.6 Detail of scalloped connection



### 3. TEST RESULTS

#### 3.1 Results of Simple Beam Specimens

The relations between the load ( $P$ ) and the beam rotation ( $\theta$ ) of the simple beam specimens are shown in Fig.8 and Fig.9. The dotted lines in these figures show the results of the bending tests performed to confirm the full plastic moment of the beam member. Fig.10 shows the relations between the beam rotation and the axial strain of the tensile flange in the vicinity of the joint.

In the case of the beams with two axes of symmetry shown in Fig.8, the elastic stiffness and the maximum strength of each specimen do not differ much from those of another. On the other hand, the smaller the thickness of column wall is, the smaller the strength is as the elastic region develops into the plastic region; the strength of the scalloped specimen is apparently smaller than that of the nonscalloped specimen. The drop in the load after the maximum strength is due to the local buckling in the flange and the web.

The same can be said about the results of the specimens with a single axis of symmetry shown in Fig.9 as far as elastic stiffness is concerned. This time, the plastic neutral axis is in the compressive flange, and as seen in Fig.10, the strain of tensile flange is considerably larger than in the case of two axes of symmetry. Further, the strain of the scalloped specimen is larger than that of the nonscalloped specimen. As a result, the scalloped specimen SB6-S-1A caused a ductile fracture in the tensile flange where it is scalloped as shown in Fig.11. On the contrary, not a crack was observed in the the nonscalloped specimens throughout the test.

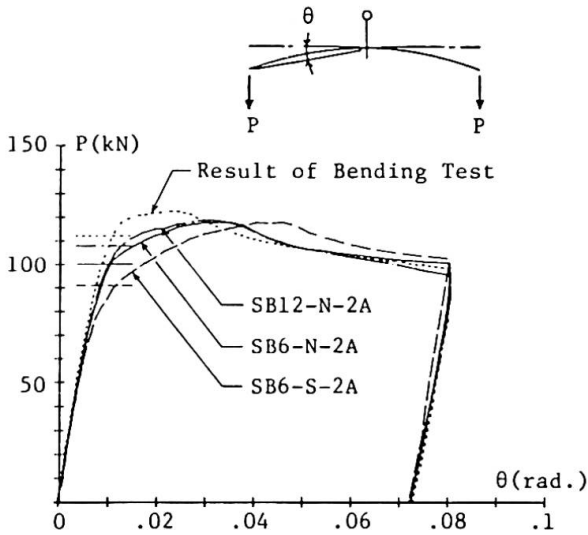


Fig.8 Simple beam with two axes of symmetry

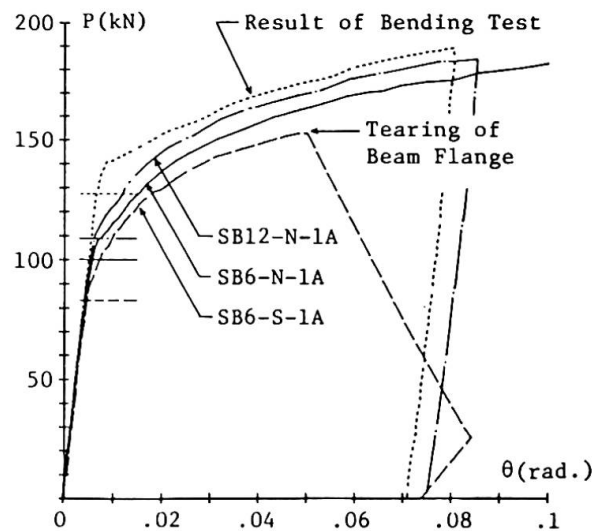


Fig.9 Simple beam with a single axis of symmetry

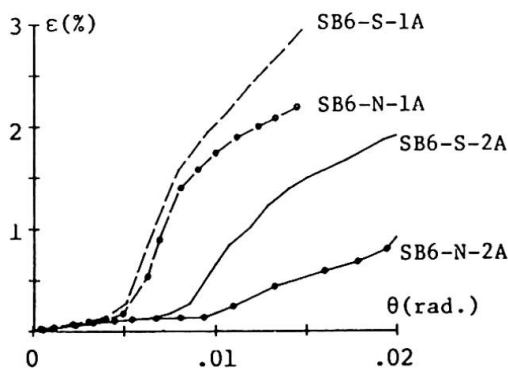


Fig.10 Axial strain of tensile flange

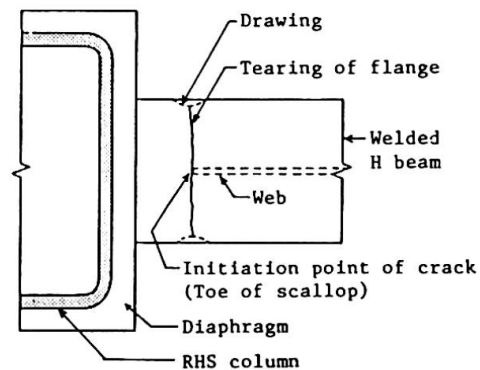


Fig.11 Tearing of tensile flange

### 3.2 Results of Cruciform Subassemblages

The relations between the column shear force ( $Q$ ) and the column rotation ( $R$ ) as in Fig.4 are shown in Fig. 12 and Fig. 13. In the case of scalloped specimen No.10, the crack that was initiated at the toe of the scallop the first loading cycle widened outward the second cycle to cause a fracture. On the other hand, as apparent from Fig.13, the nonscalloped specimen No.11 showed a sufficient deformability without any cracks under the repeated loading, the strength of which however decreased due to local bucklings.

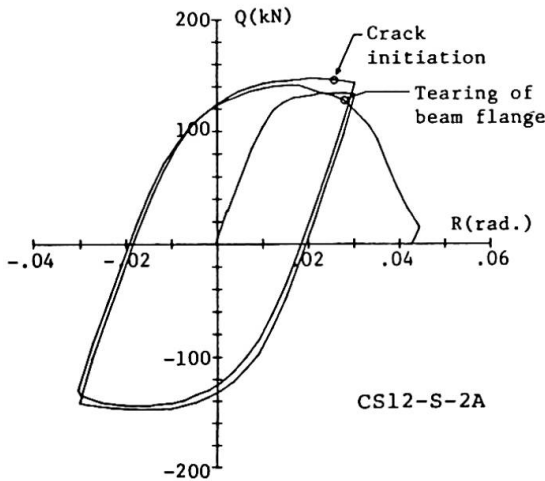


Fig.12 Q-R relation of cruciform subassemblage (with scallop)

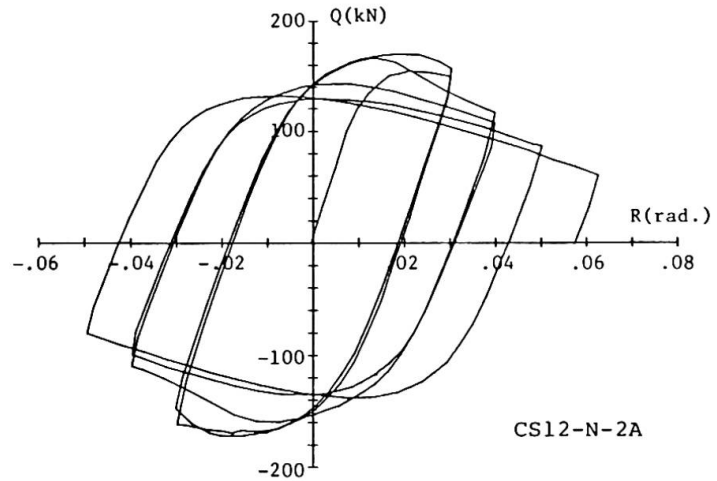


Fig.13 Q-R relation of cruciform subassemblage (without scallop)

### 4. COMPARISON OF THE TEST RESULTS WITH CALCULATED RESULTS

As shown in Fig.8 and Fig.9, the flexural strength of the beams connected to an RHS column is smaller than in the bending test. This is due to the external deformation of the column tube wall to which the beam web is connected. As an example, the distribution of web strain in the simple beam specimen (No.8) at  $\theta = 0.02$  rad. and the surface contour map of a deformed column wall after testing are shown in Fig.14.

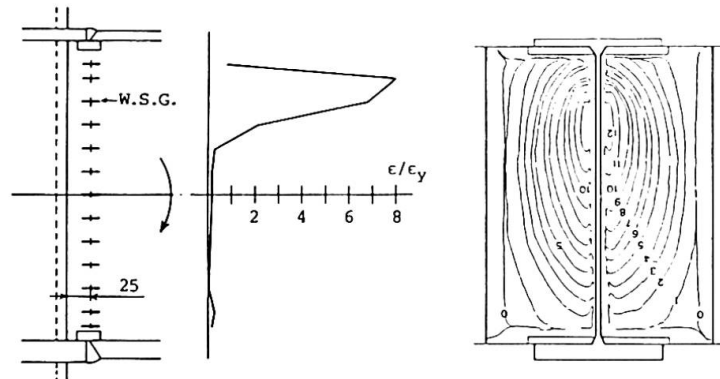


Fig.14 Strain distribution and surface contour map of column tube wall

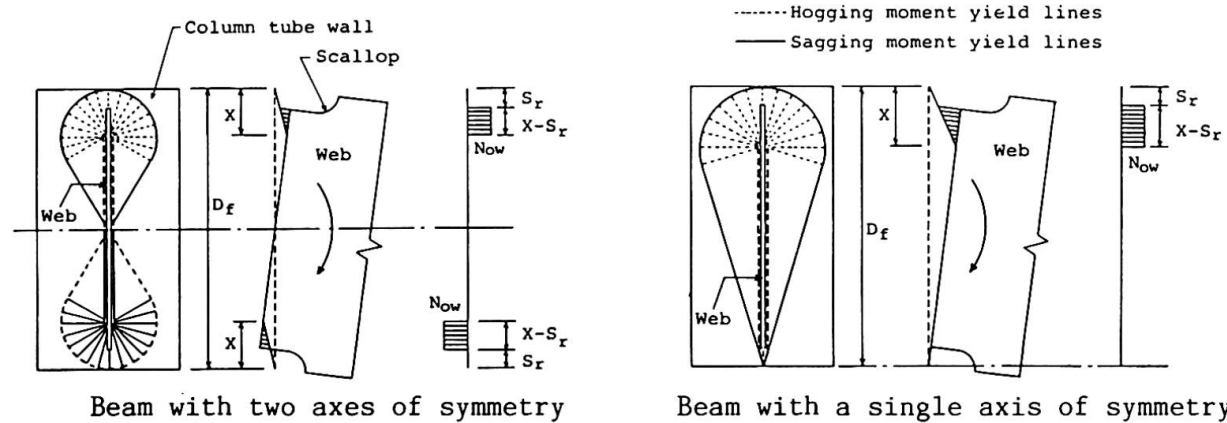


Fig.15 Mechanism of column tube wall and assumed stress distribution of beam web



The collapse mechanisms of column tube wall are assumed as shown in Fig.15. The moment transmitted through the beam web can be calculated by using the yield line theory [3,4]. The detailed derivative processes of the equations are omitted here. The length (X) of the plastic region of the web as in Fig.15 can be given approximately by the following equations:

$$\text{Section with two axes of symmetry:} \quad X = \sqrt{\frac{4D_f M_{ot}}{N_{ow}}} \quad (1)$$

$$\text{Section with a single axis of symmetry:} \quad X = \sqrt{\frac{8D_f M_{ot}}{N_{ow}}} \quad (2)$$

where  $M_{ot}$  is the full plastic moment per unit width of the column tube wall and  $N_{ow}$  is the yield axial force per unit width of the beam web or the punching shear strength of tube wall. If it is assumed that the yield stress acts only on the area of the web hatched in Fig.15 and the stress of the remaining area of the web is nil, the collapse moment of the beam at the joint can be calculated using the value of X obtained from the above equations. In Fig.15,  $S_r$  is the depth of the scallop, and in case of nonscallop,  $S_r = 0$ .

The horizontal lines in Fig.8 and Fig.9 show the collapse load levels of individual test specimens calculated by the above method. The calculated collapse load of each specimen is close to the corresponding load level at which the gradient of P- $\theta$  relations greatly decreases.

## 6. CONCLUSION

From the test results, it has been confirmed that the nonscallop detail shown in Fig.7 has the following advantages over the conventional scalloped connections.

- (1)The deformability of the beam is greatly improved.
- (2)The flexural strength of the beam as the elastic region advances into the plastic region increases approximately by 10%.
- (3)It can save the cost of fabricating the connections by not using scallops.

We may also mention here that the flexural strength of wide flange steel beams connected to RHS columns becomes smaller than their full plastic moment as a result of the external deformation of the column tube wall. The flexural strength can be predicted by the present method based on the yield line theory.

## ACKNOWLEDGMENTS

The authors would like to acknowledge the continuing guidance and encouragement of Professor Sadayoshi Igarashi of Osaka University.

## REFERENCES

1. FUJIMOTO M. et al, Experimental Study on the Brittle Fracture of Beam-to-Column Welded connections in Heavy Members Steel Structures, Part 1. J. of Structural and Construction Eng., Trans. of AIJ, No.349, pp.81-90, 1985.
2. KANATANI H. et al, Rigidity and Strength of Joint Panel of Centrifugally Cast Steel Tubular Column, Trans. of Annual Meeting of AIJ, pp.921-922, 1985.
3. MANSFIELD E. H., Studies in Collapse Analysis of Rigid-Plastic Plates with Square Yield Diagram. Proc. of the Royal Society London, 241, Series A, pp.311-338, Aug., 1957.
4. DAVIES G. and PACKER J. A., Predicting the strength of branch plate-RHS connections for punching shear. Can. J. Civ. Eng., Vol.9, No.3, pp.458-467, 1982.